Polymer Journal, Vol. 20, No. 6, pp 447—457 (1988)

Some Characteristic Features of Dilute Aqueous Alkali Solutions of Specific Alkali Concentration (2.5 mol l^{-1}) Which Possess Maximum Solubility Power against Cellulose

Takashi YAMASHIKI, Kenji KAMIDE,* Kunihiko OKAJIMA, Keisuke KOWSAKA, Toshihiko MATSUI, and Hiroko FUKASE

Fundamental Research Laboratory of Fibers and Fiber-Forming Polymers, Asahi Chemical Industry Co., Ltd., 11-7 Hacchonawate, Takatsuki, Osaka 569, Japan

(Received November 18, 1987)

ABSTRACT: Some structural features of aqueous (aq.) alkali solutions with specific concentration (2.5 mol l^{-1}), in which cellulose shows maximum swelling or dissolution, were investigated by analysing electrical conductivity, ^{1}H and ^{23}Na NMR, solvation and Raman spectra of aq. alkali, especially aq. sodium hydroxide. Cellobiose solution in aq. alkali was also subjected to ^{1}H NMR and specific rotatory angle measurements to elucidate the dissolved state of cellulose. It was found that in the specific alkali concentration, electrical conductivity, ^{1}H and ^{23}Na chemical shifts and ^{1}H relaxation time became smaller and the number of solvated water molecules per 1 mole of alkali hydroxide became larger than those simply expected from their alkali concentration dependence in the outside range of specific alkali concentration. Raman spectra revealed that the peak giving maximum intensity of OH-deformation is energetically weakest at the specific concentration of aq. alkali. When cellobiose was added to the aq. alkali solution it was found that proton chemical shift of the system becomes larger especially at 4°C over the all alkali concentration range and its dependence on alkali concentration was almost linear. Based on these experimental facts some structure models of aq. alkali solution with specific concentration and the dissolved state of cellulose in the alkali solution were proposed.

KEY WORDS Aqueous Alkali Solution / Specific Concentration / ^{1}H NMR / ^{23}Na NMR / Electrical Conductivity / Solvation / Raman Spectra / Cellulose /

For many years it has been widely known that natural or regenerated cellulose swell at least partially in aqueous (aq.) alkali solutions. In this case cellulose shows maximum swelling at a specific concentration of aq. alkali solution: 8—10 wt% for aq. sodium hydroxide (NaOH) and 5—10 wt% for aq. lithium hydroxide (LiOH) at comparatively lower temperature.[1-6] Recently, Kamide *et al.* demonstrated that cellulose samples, regenerated under certain conditions, can completely dissolve in 8—10 wt% aq. NaOH solution at 4°C and in 6 wt% aq. LiOH.[7] They successfully correlated the solubility of cellulose in aq. alkali solution with the degree of break-down of an intramolecular hydrogen bond ($O_3 \cdots O_5'$) of cellulose as determined by CP/MAS ^{13}C NMR method.[7] Natural cellulose, if exploded or extruded after treatment with water under high pressure for a relatively

* To whom all correspondence should be addressed.

short time,[8-10] can also dissolve perfectly into aq. NaOH solution below 7°C. The alkaline solubility of the treated natural cellulose is also closely correlated with the degree of break-down of an intramolecular hydrogen bond[11] and it seemes that almost complete dissolution of cellulose into aq. alkali with specific concentration at low temperature requires the break-down of intramolecular hydrogen bond at C_3 and C_6, as determined by CP/MAS ^{13}C NMR, by at least 45%. Therefore, one of the most important factors controlling the maximum swelling or solubility of cellulose in aq. alkali solution at specific alkaline concentration is the structure of the aq. alkali solution.

In this article, we report some structural characteristics of aq. alkali solutions with specific concentration, in which the maximum swelling or maximum solubility of cellulose is attained, and propose a tentative structure of cellulose/aq. alkali solution systems.

EXPERIMENTAL

Materials

Guaranteed grade NaOH and LiOH, both supplied by Wako Jun-yaku Co. (Japan) were used as recieved. Aq. alkali solutions were prepared by dissolving the alkalis in purified water (Aoi Jun-yaku Co., Japan). An alkali-soluble pulp having cellulose I crystal (the viscosity-average degree of polymerization $DP_v=380$, determined from the Mark–Houwink–Sakurada equation established for cellulose/cadoxen system[12] and the degree of break-down of intramolecular hydrogen bond at C_3 and C_6 $\chi_{NMR}(C_3+C_6)=48$, determined by CP/MAS ^{13}C NMR) was prepared by physical treatment[8-10] to break-down the intramolecular hydrogen bond to some extent and employed for the further dissolving test. As a cellulose model compound cellobiose (supplied by Kishida Chemicals Co., Ltd., Japan) was also utilized for ^1H and ^{23}Na NMR and the specific rotatory angle measurements.

Measurements

The solubility of cellulose in aq. NaOH and LiOH solutions S_a was measured as follows: 5.43 grams (g) of cellulose (water content 8 wt%) were dispersed in 95 g of a given concentration of aq. alkali, precooled at 4°C, stood for 8 h with occasionally mixing with home mixer and the insoluble part was separated by centrifuging at 3,000 rpm for 20 min. The insoluble part was neutralized with hydrochloric acid to precipitate the cellulose completely. The cellulose was washed with water, dried first in air and finally *in vacuo* and weighed (w g). S_a was defined as $100\times(5-w)/5(\%)$.

Electrical conductivity σ was measured for aq. alkali as functions of alkali concentration C_a and temperature on a Conduct-O-meter model CM-2A (Toa Denpa Co., Japan).

^1H and ^{23}Na NMR spectra were recorded for various aq. alkali solutions on a FX-200 type FT-NMR spectrometer (JEOL, Japan) with multi-nuclei measurement system, in a C/H 10 mmϕ probe and a tunable 10 mmϕ probe, respectively. For this purpose, a co-axially centered sample tube was employed for FT-NMR measurements; Deuterium oxide (D_2O) as external lock signal was placed in the outer tube and aq. alkali solution sample was placed in the internal tube. Various cellobiose/aq. alkali systems (20 g of cellobiose in 100 g of aq. alkali) were also subjected to ^1H and ^{23}Na NMR measurements. Operating conditions used are as follows:

^1H : Frequency 199.5 MHz, flip angle $\pi/2$, pulse interval 5 s, internal reference trimethylsilylpropionic acid sodium salt (TSP).

^{23}Na: Frequency 52.8 MHz, flip angle $\pi/2$, pulse interval 5 s, external reference sodium chloride.

For evaluating spin-lattice relaxation time T_1 of the ^1H and ^{23}Na peaks of aq. alkali so-

lutions the peak intensity A_τ at given pulse interval τ was measured using a π–τ–$\pi/2$ FID pulse sequence and T_1 was calculated from the following equation by the inversion-recovery method:

$$\tau/T_1 = -\ln\{(A_{20s}-A_\tau)/2A_{20s}\} \qquad (1)$$

where A_{20s} and A_τ mean peak intensities at $\tau=$ 20 s and τ, respectively.

The optical rotatory angle α was measured as function of C_a and temperature for various cellobiose/aq. alkali systems (20 g of cellobiose in 100 g of aq. alkali) at the wave number of the incident light $\lambda=436$ nm (Hg lamp) by a DIP 181 type instrument (Nihon Bunkou Co., Japan). α for these systems has proved to decrease with time, obeying almost first order kinetics and therefore, the measurements, which required 2 s, were done 2.5 minutes after the solution preparation. Specific rotatory angle $[\theta]$ was calculated from α using the relation $[\theta]=\alpha/(l\cdot c)$, where l and c represent the length of the pass (cm) and cellobiose concentration (mol dl^{-1}).

Raman spectra were recorded for aq. alkali solutions with various C_a on a spectrophotometer (JRS-400D Laser Raman Spectrophotometer, JOEL, Japan) at room temperature. Laser light with $\lambda=541.5$ nm generated under 150 mW was passed through the sample solution and the intensity of the vertically scattered Raman light was recorded. Half value width $\Delta_{1/2}$ of the Raman absorption band in question was determined as follows: For OH stretching a base line was set between 3800 cm $^{-1}$ and 2400 cm^{-1} and from the peak having maximum intensity of scattered Raman light (point P) a straight line parallel to intensity axis was drawn on the base line. The crossing point was denoted as O. A straight line parallel to the base line passing through the middle point of line PO was drawn and the wave number at the crossing points (M and N) with the peak in question was determined. Difference in the wave number at M and N was regarded as $\Delta_{1/2}$ (see Figure 7). For OH deformation, the procedure was the same as that described above except that a base line was set between 1800 cm^{-1} and 1550 cm^{-1}.

Sound velocity v was measured with a Pierce type ultrasonic interferometer, constructed by Nomura and Miyahara,[13] operating at 4.999985 MHz. The temperature of the solution was controlled to ± 0.005°C by circulating water around the cell of the interferometer. The density ρ of the solution was measured with an Ostwald type pycnometer. The adiabatic compressibility β was calculated by the Laplace equation.

$$\beta = 1/(\rho v^2) \qquad (2)$$

The number of solvated water molecules per 1 mol of alkali (NaOH) S was calculated using Passynsky's equation[14]:

$$S=(1-\beta/\beta_s)(100\rho - C_a')/C_a' \qquad (3)$$

Here, β_s denotes the adiabatic compressibility of water and C_a', the concentration of the alkali expressed in mol l^{-1}.

RESULTS

Figure 1 shows the solubility S_a of a cellulose sample at 4°C as a function of alkali concentration C_a. S_a was found to attain almost 100% at specific concentrations of aq. LiOH (about 5.8 wt%) and NaOH (about 9 wt%) solutions. These two concentrations, interestingly fall on about 2.5 mol l^{-1}. We believe these are the first experimental results demonstrating that cellulose having crystal form I dissolves completely in aq. alkali solution, if the intramolecular hydrogen bond of cellulose sample is appropriately broken down in advance.

Figure 2 shows the electrical conductivity σ (expressed in SI unit $10^{-1}\,\Omega^{-1}\,m^{-1}$) of aq. solution of NaOH (a) and LiOH (b) plotted against the concentration of alkali C_a at a given temperature. The positive C_a and temperature dependences of $\sigma(\partial\sigma/\partial C_a \geqq 0$ and $\partial\sigma/\partial T>0)$ were observed over the C_a range 0–

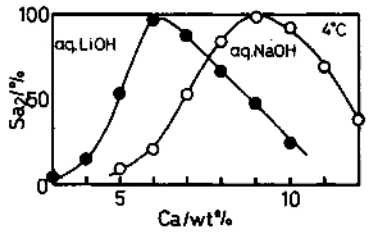

Figure 1. Solubility S_a of cellulose at 4°C as a function of alkali concentration C_a: ○, aq. NaOH; ●, aq. LiOH.

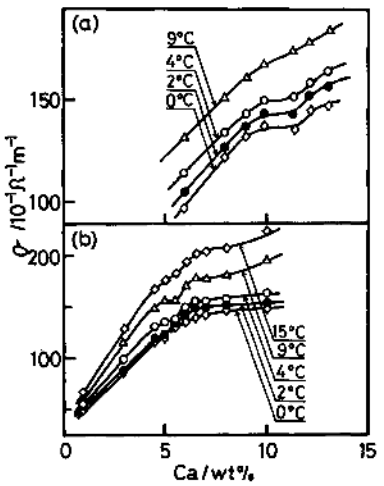

Figure 2. Dependence of electrical conductivity σ of aq. solution of NaOH (a) and LiOH (b) on alkali concentration C_a.

15 wt%. However, the gradient of σ *vs.* C_a plot became nearly zero in *ca.* 9–12 wt% of aq. NaOH in a lower temperature range, where cellulose exhibited the maximum swelling or solubility. Aq. LiOH exhibited the same phenomena.

Figures 3a and b show the proton chemical shift δ_H (a) and ^1H spin-lattice relaxation rate $1/T_{1H}$ (b) of aq. NaOH solutions as a function of C_a at 4°C (circle) and 10°C (triangle), respectively. The figure also contains the data (closed symbols) for a cellobiose solution in these alkali. C_a dependence of δ_H is almost the same but its temperature dependence is reserved as observed for σ–C_a relation. Contrarily, $1/T_{1H}$ of aq. NaOH exhibits a remarkable sharp increase in almost the same

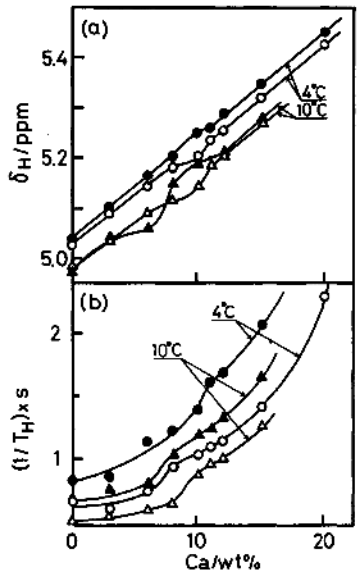

Figure 3. Dependence of proton chemical shift δ_H (a) and ^1H spin-lattice relaxation rate $1/T_{1H}$ (b) of aq. NaOH solutions and cellobiose/aq. NaOH system on alkali concentration C_a: ○, aq. NaOH at 4°C; ●, cellobiose/aq. NaOH at 4°C; △, aq. NaOH at 10°C; ▲, cellobiose/aq. NaOH at 10°C.

C_a region observed for δ_H–C_a relation. When cellobiose was added, a gradient of δ_H *vs.* C_a plot increased abruptly approaching nearly zero in the above plateau region and the region of sharp $1/T_{1H}$ increase shifted to higher C_a at 4°C and to lower C_a at 10°C. Both δ_H and $1/T_{1H}$ values of the cellobiose/aq. NaOH system at 4°C were always higher than those of aq. NaOH at 10°C over all C_a region.

Figures 4a and b show ^{23}Na chemical shift δ_{Na} (a) and ^{23}Na spin-lattice relaxation rate $1/T_{1Na}$ of aq. NaOH (b) as a function of C_a at 4°C. δ_{Na} shows a similar C_a dependence on that observed for δ_H: A reflection point appeared in the C_a range 8—14 wt%. When cellobiose was added, δ_{Na} almost linearly increased with C_a and δ_{Na} values below $C_a = 8$ wt% were almost equal to those for the aq. NaOH system. $1/T_{1Na}$ values for both aq. NaOH and cellobiose/aq. NaOH systems increased monotonically with an increase in C_a over entire C_a range examined, but the absolute value for the latter

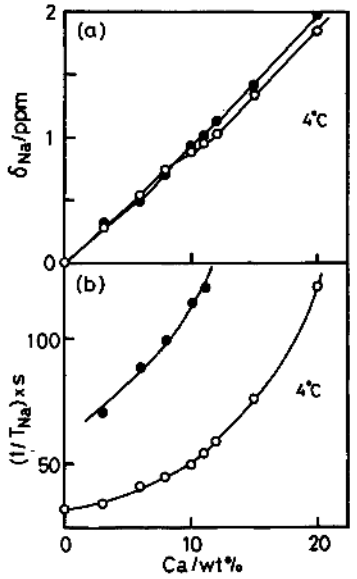

Figure 4. Dependence of ^{23}Na chemical shift δ_{Na} (a) and ^{23}Na spin-lattice relaxation rate $1/T_{1Na}$ of aq. NaOH at 4°C on alkali concentration C_a: ○, aq. NaOH; ●, cellobiose/aq. NaOH.

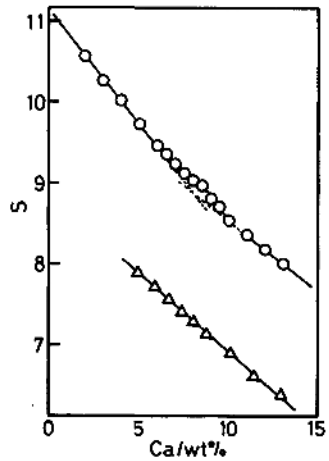

Figure 5. Number of water molecules solvated to an NaOH molecule S as a function of alkali concentration C_a: ○, 4°C; △, 20°C.

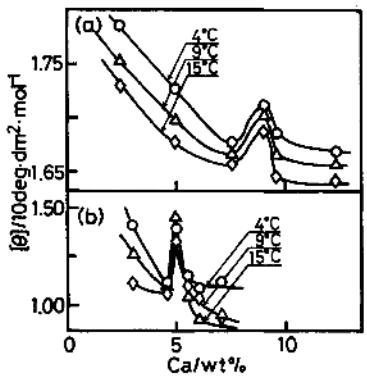

Figure 6. Dependence of the specific rotatory angle $[\theta]$ of the cellobiose/aq. alkali systems on alkali concentration C_a: Numbers on the lines denote temperature.

system is considerably larger than that for the former system. Absolute $1/T_{1Na}$ was found to be far larger than $1/T_{1H}$.

Figure 5 shows the number of water molecules solvated to an NaOH molecule S as a function of C_a at 4°C (open circle) and 20°C (open triangle). S generally decreased linearly with increasing in C_a at 20°C. But, C_a dependence of S at 4°C was roughly approximated with two linear lines above 11 wt% and below 6 wt% with different slopes. A significant deviation from these two lines attained maximum at $C_a=8$—9 wt%. It can be concluded that one mole of NaOH solvates with about 8—9 mol of water, which is larger by about 0.2 mol than the value expected from the two linear C_a dependence lines, over the C_a range 8—10 wt% at 4°C.

Figure 6 shows the specific rotatory angle $[\theta]$ of the cellobiose/aq. alkali systems as a function of C_a at 4, 9, and 15°C. $[\theta]$ seems to decrease with increasing C_a but exhibits a relatively sharp peak at $C_a=9$ wt% for aq. NaOH and 5 wt% for aq. LiOH. Absolute $[\theta]$ value was always higher at lower temperature, when compared at same C_a level.

Figures 7a and b show the Raman spectra in the OH-stretching and -deformation regions for aq. NaOH with various C_a, respectively. The maximum scattering peak positions and the spectra shapes change remarkably depending on C_a: In the OH-stretching region, the shoulder peak located at higher wavenumber region in the maximum peak became weak

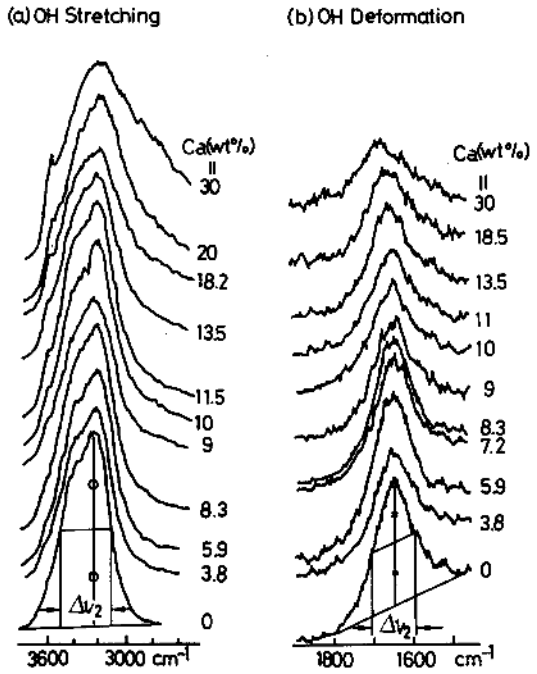

Figure 7. Raman spectra in the OH-stretching (a) and -deformation (b) regions for aq. NaOH: Numbers on the lines denote C_a (wt%).

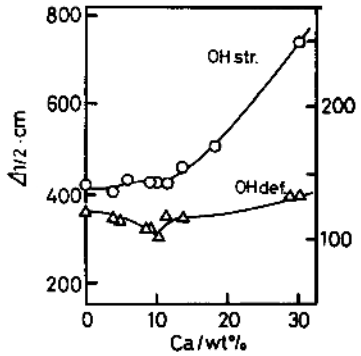

Figure 8. Dependence of the half value width $\Delta_{1/2}$ of scattering peaks for OH-stretching region (○) and OH-deformation region (△) on alkali concentration C_a complicated when C_a is around 7—9 wt%.

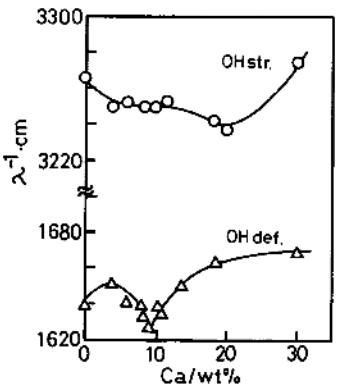

Figure 9. Dependence of the maximum peak position (wave number λ) in the OH-stretching (○) and OH-deformation (△) on C_a.

over C_a range 8—9 wt% and again became distinct in C_a range 10—11.5 wt%. In the OH-deformation region, the shape of peaks is very complicated when C_a is around 7—9 wt%.

In Figure 8 the half value widths $\Delta_{1/2}$ of scattering peaks for OH-stretching region and OH-deformation region are plotted against C_a. In the OH-stretching region $\Delta_{1/2}$ remained practically constant up to *ca.* 10 wt%, and in particular, in range 5—11 wt%. $\Delta_{1/2}$ increased linearly with an increase in C_a in the range $C_a > 11$ wt%. In contrast to this, in OH-deformation, a gradual decrease of $\Delta_{1/2}$ was observed for $C_a < 10$ wt% and $\Delta_{1/2}$ increased slightly after passing a minimum $\Delta_{1/2}$ at $C_a = 8$—10 wt%.

Figure 9 shows the dependence of wavenumbers at peak $1/\lambda$ corresponding to the OH-stretching (denoted as circle) and the OH-deformation (denoted as triangle) on C_a. The $1/\lambda$ of the OH-stretching decreased with increase of C_a until $C_a = 20$ wt% and after passing through minimum increased much. The peak position of OH-deformation clearly shows a minimum at $C_a = 9$ wt%. The shift width for the peak position giving a maximum intensity for OH deformation range amounts to as much as 40 cm^{-1}. For example, the above-mentioned peak appeared at 1627 cm^{-1} and 1670 cm^{-1} at $C_a = 9$ and 30 wt%, respectively. The former peak is also located at a considerably lower wave number, compared with that for pure water (1640 cm^{-1}).

Table I. Specific features observed for aq. NaOH and LiOH solutions

Physical properties	Temp	Specific C_a range/wt%		Figures	Remarks
	°C	NaOH	LiOH		
Solubility of cellulose (S_a)	4	9.0	5.8	Figure 1	
Electrical conductivity (σ)	0–15	9.0—12.0	4.5—6.0	Figure 2	Low cationization of Na^+
^1H Chemical shift of H_2O (δ_H)	4	7.5—12.0		Figure 3a	Weak hydrogen bond of OH^-
	10	7.5—12.0			
^1H Chemical shift of H_2O with cellobiose (δ_H)	4	8.0—11.0		Figure 3a	Strong hydrogen bond of cellobiose
	10	7.5—12.0			
^1H Spin-lattice relaxation rate of H_2O ($1/T_{1H}$)	4	6.5—8.0		Figure 3b	Strong interaction (hydrogen bond) of OH^-
	10	8.0—10.0			
^1H Spin-lattice relaxation rate of H_2O with cellobiose	4	10.0—12.0		Figure 3b	Strong hydrogen bond of cellobiose
	10	7.0—9.0			
^{23}Na Chemical shift of Na^+ (δ_{Na})	4	8.0—14.0		Figure 4a	Weak hydrogen bond of Na^+
^{23}Na Spin-lattice relaxation rate of NaOH ($1/T_{1Na}$)	4	—		Figure 4b	
Solvated water molecules (S)	4	8.0—9.0		Figure 5	Extra solvated H_2O molecules
	20	—			
Specific rotatory angle of cellobiose ($[\theta]$)	4—15	9.0	5.0	Figure 6	Specific configuration of cellobiose
HVW of Raman peaks ($\Delta_{1/2}$)				Figure 8	
(–OH stretching)	25	—			
(–OH deformation)	25	8.0—10.0			Long life time
Wavenumber of Raman peaks (λ)				Figure 9	
(–OH stretching)	25	—			
(–OH deformation)	25	9.0			Weak hydrogen bond

DISCUSSION

The characteristic features of aq. alkali solutions observed in this study are summarized in Table I. The experimental facts observed here point out that one of the most important factors controlling the dissolution of the cellulose, whose intramolecular hydrogen bond has been adequately broken, into aq. alkali is the structure of the alkali with specific concentration. Therefore, it is useful to clarify its structure. Hereafter, emphasis is placed on aq. NaOH.

In the C_a and temperature range where cellulose shows maximum swelling or dissolution, σ is around $130-150\,m\Omega^{-1}\,cm^{-1}$, irrespective of alkali species. However, an explicit appearance of plateau region (about $2.5\,mol\,l^{-1}$) in σ–C_a relations (Figure 2) implies that there is some metastable state which restricts to some extent ionic transportation. The restriction of ionic transportation means that the degree of cationization or anionization of the masses in the system is smaller than those simply expected from their C_a dependence in the outside of the plateau region. A higher absolute σ value at higher temperature is probably due to a larger dissociation constant of the system at higher temperature.

H^+ and OH^- in H_2O and NaOH exchange rapidly, so that we can not distinguish these hydrogen species separately only knowing the time-average state. Two different physical meanings of proton chemical shift δ_H can be considered: δ_H is a measure of the average hydrogen bond strength or the degree of cationization of the hydrogen: In the first case, it is expected that the higher the δ_H, the stronger is the hydrogen bond. The plateau

region of the δ_H *vs.* C_a plot suggests the existence of a state where the strength of the hydrogen bonds of the system became less than the value extraporated from the experimental relation in the region of C_a below 7.5 wt% or more than 12 wt%. In the second case, cationization of hydrogen, judging from the results for δ_H, should be higher at lower temperature, which is in sharp contrast to the results obtained by electrical conductivity measurements. Thus, a simple cationization concept cannot be accepted. The existance of plateau region for T_{1H} in the same C_a region observed for δ_H is an indication that a rotational motion of the proton as a whole is more or less restricted and the life time of a given state is shortened more than anticipated from the extrapolation of experimental T_{1H} C_a relations below $C_a=7.5$ wt%. In other words, in this C_a region, a proton excited by an NMR field more easily transfer its energy to the lattice (for example, surrounding H_2O molecules). Therefore, it is probably true to say that if cellulose is added to the aq. NaOH solution with a specific concentration, cellulose can easily accept energy from the system.

^{23}Na chemical shift δ_{Na} *vs.* C_a plot reveals again a small plateau as observed for δ_H. The over-all absolute value of δ_{Na} at 10°C, obtained in a separate experiment, was almost equal to that at 4°C at same C_a, showing that δ_{Na} is independent of temperature. Then, it is conceivable that δ_{Na} is not a measure of the degree of cationization but a measure of the degree of hydrogen bond strength of the whole system made through interactions of the solvated water molecules. Since $1/T_{1Na}$ monotonically increases with C_a, the system has no specific state where ^{23}Na excited by an NMR field more easily transfers its energy to the lattice in a specified C_a range. The life time of Na^+ in a given ionic structure is far shorter than that of H^+, judging from $1/T_{1Na}$ and $1/T_{1H}$. It is obvious therefore that Na ion does not play a very important role in the dissolution of cellulose in aq. alkali.

The number of solvated water molecules on Na^+ in the C_a range 6—11 wt% is slightly larger (about 0.2 mol/mol of NaOH) than that extrapolated from the experimental relations over the range of C_a below 6 wt% and more than 11 wt%. This explains the results obtained for σ, δ_H, T_{1H}, and δ_{Na}. Solvation of extra water molecules on the totally cationized or anionized mass (Na^+ or OH^- solvated with a definite number of water molecules) through hydrogen bonding may decrease its cationic density and weaken the hydrogen bond, resulting in a decreasing of σ and δ_H. In this connection, H^+ and OH^- ions in solvated water molecules are to some extent mutually interchangeable and can also easily interchange with free water molecules. The extra solvated water then makes weak hydrogen bonds against original free water in the system and this leads to decrease in T_{1H} of the system through dipole–dipole interactions between OH^- and H^+. The extra solvated water molecules can thus act as an energy transfer media between the masses and free water.

The experimental results for the half value widths of the maximum Raman peak $\Delta_{1/2}$ of OH-stretching and -deformation indicate that these vibration states have longer life time at $C_a<10$ wt% than those at $C_a>10$ wt%. But, similar results on the maximum Raman peak $1/\lambda$ of the OH-deformation suggest that the strength of hydrogen bond formed in the direction of OH-deformation vibration is weakest at $C_a=9$—10 wt%. Raman spectra due to the OH-deformation reveal that there are several OH vibration states, each having a different strength of hydrogen bond at $C_a=$ 7—10 wt%. These results are very comparable to the results on σ, δ_H, T_{1H}, and S.

When cellobiose as cellulose model is added into aq. alkali solution, the total strength of the hydrogen bond of the system becomes greater as judged from an increase in δ_H and this tendency is somewhat more in the specified C_a range where cellulose shows maximum dissolution. At 4°C, where cellulose shows

more preferred dissolution than at 10°C,[15] T_{1H} *vs.*C_a plot gives almost a linear relationship over the all C_a region, excluding the existence of the specific C_a region observed for aq. alkali system without cellobiose. This means that cellobiose takes part in hydrogen bond formation with the cationized or anionized mass strongly solvated with water excluding a part of the extra solvated water molecules. In this connection, an acid-base reaction concept for the dissolution of cellulose can be denied because if such a reaction should take place, δ_H would decrease reflecting a decrease in the strength of base. The existence of cellobiose in the system also lowers T_{1H}, suggesting that cellobiose can easily form hydrogen bonds

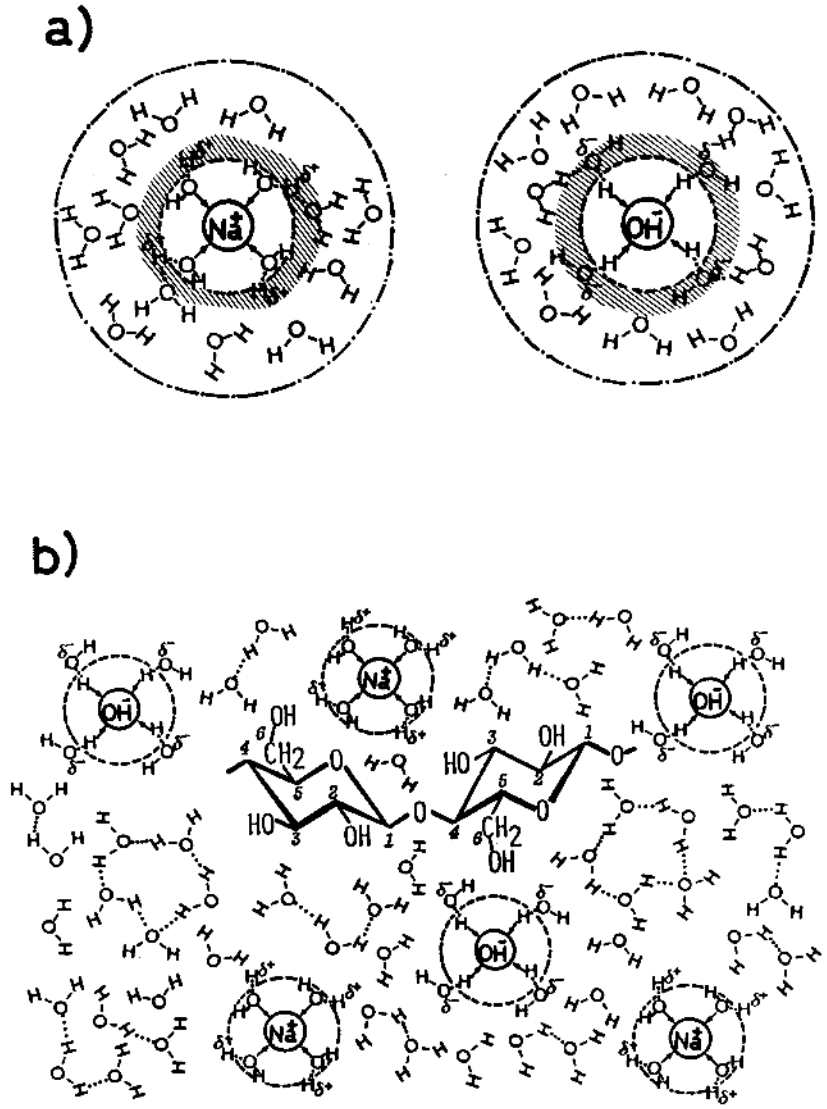

Figure 10. Schematic representation of tentative structure of aq. NaOH solution with specific concentration (9 wt%) and the dissolution state of cellulose in the system.

with surrounding water resulting in a shorter life time of the existing state of the proton in the total system. The use of cellobiose as cellulose model is reasonable since we discuss only a time-average state of the system induced by the change in total hydrogen bonds.

It is not clear at present whether the abrupt increase in specific rotatory angle [θ] of cellobiose/aq. alkali solution systems in the specific C_a range suggests that cellobiose takes a specific conformation in the system. However, if so, the aq. alkali with specific concentration may have some specific interaction with intramolecular hydrogen bond in cellobiose.

In the sixth column of Table I, the above discussions are briefly given as remarks. A tentative structure of aq. NaOH solution with specific concentration (9 wt%) and a dissolved state of cellulose in the system are illustrated in Figure 10. Total 8 mol of water solvate with a Na^+ ion and a OH^- ion (i.e., 4 mol/each ion) forming the cationic and anionic masses, respectively. Around these masses 0.2 mol of water on the average forms the 2nd solvation area (extra water solvation area) and the outer of the area is surrounded by about 22.8 mol of free water. Since any cellulose will swell considerably by the alkali and be converted to alkali cellulose, intermolecular hydrogen bonds might be raptured easily. For the complete dissolution of cellulose, the breakdown of intramolecular hydrogen bond to some extent is the minimum necessary condition. In the first approximation, the interactions of aq. alkali with specific concentration with OH groups in cellulose, which do not participate in intramolecular hydrogen bond might determine the dissolution of cellulose into the aq. alkali. Thus, as shown in Figure 10, cellulose strongly interacts with both cationic and anionic masses and also forms relatively strong hydrogen bonds with free water originally existing in aq. NaOH. The free water has some tendency to make hydrogen bonds with each other through interaction between cellulose and the ionic masses. In this process, it is plausible to consider that the existence of 2nd solvation layer in original aq. NaOH solution may play a very important role in maintaining the electrical and hydrogen bonding nature of the system and in replacing the layer with cellulose.

Na cations do not directly play an important role in the dissolution of cellulose and this has been proved by Kamide *et al.*,[16] who experimentally verified that Na ions did not show affiliation to the specific OH of cellulose in its aq. alkali solution and in contrast to this, the "so-called alkali cellulose" has Na ions to the OH group at the C_2 position of a glucopyranose unit.

Summarizing, we confirmed the existence of the structure of aq. alkali solution with specific alkali concentration (2.5 mol l^{-1}) in which cellulose shows maximum swelling or maximum dissolution, by analysing the alkali concentration dependence of electrical conductivity, ^1H and ^{23}Na NMR, solvation and Raman spectra of aq. alkali.

REFERENCES

1. C. Beadle and H. P. Stevens, The 8th International Congress on Applied Chemistry, Vol. 13, 1912, p 25.
2. S. M. Neals, *J. Text. Inst.*, **20**, T373 (1920).
3. H. Dillenius, *Kunstseide Zellwolle*, **22**, 314 (1940).
4. H. Staudinger and R. Mohr, *J. Prakt. Chem.*, **158**, 233 (1941).
5. E. Schwart and W. Zimmerman, *Melliands Textilber. Inst.*, **22**, 525 (1941).
6. O. Eisenluth, *Cellulose Chem.*, **19**, 45 (1941).
7. K. Kamide, K. Okajima, T. Matsui, and K. Kowsaka, *Polym. J.*, **16**, 857 (1984).
8. T. Yamashiki, T. Matsui, M. Saito, K. Okajima, and K. Kamide, *Cellulose Chem. Tech.*, to be submitted.
9. T. Yamashiki, T. Matsui, M. Saito, K. Okajima, and K. Kamide, *Cellulose Chem. Tech.*, to be submitted.
10. T. Yamashiki, T. Matsui, K. Kowsaka, M. Saito, K. Okajima, and K. Kamide, *Cellulose Chem. Tech.*, to be submitted.
11. K. Kamide and K. Okajima, US Patent, 4634470 (1986).
12. W. Brown and R. Wikström, *Eur. Polym. J.*, **1**, 1 (1966).
13. Y. Miyahara and Y. Matsuda, *J. Chem. Soc. Jpn., Pure Chem. Sect.*, **81**, 692 (1960).

14. A. Passynsky, *Acta Physicochem. USSR*, **22**, 137 (1947).
15. K. Kamide and T. Matsui, unpublished results.
16. K. Kamide, K. Kowsaka, and K. Okajima, *Polym. J.*, **17**, 707 (1985).